

## A first glimpse of Rayleigh–Taylor, Richtmyer–Meshkov, and Kelvin–Helmholtz instabilities

A common feature during the evolutions of Rayleigh–Taylor (RT) and Richtmyer–Meshkov (RM) instabilities is the formation of a characteristic mushroom shape. Figure 1.1 shows cirrus clouds, where such beautiful structures can be observed along the lower edge of the cloud. In fact, the concept of the Rayleigh–Taylor instability (RTI) was born when Lord Rayleigh’s interest was sparked by observations of cirrus cloud formation (Jevons, 1857). He derived the properties of an interface instability that occurs when a dense fluid is supported by a lighter one (Rayleigh, 1883).

Lord Rayleigh, John William Strutt, 3rd Baron Rayleigh, made seminal contributions to many areas of physics and introduced a number of fluid dynamics concepts bearing his name. More than a century ago, it became clear to scientists in general and applied mathematicians in particular, that it would be prudent, before ever publishing any of their research, to first check whether it had not already been done by Lord Rayleigh (Gillis, 1962). He was awarded the 1904 Nobel Prize in Physics “for his investigations of the densities of the most important gases and for his discovery of argon in connection with these studies.”

According to an account by Professor J.S. Turner, the modern contribution of Sir Geoffrey I. Taylor arose from his observation and interpretation of the surface effect of an underwater explosion: the sudden appearance, then equally sudden disappearance, of an expanding dark circle (Turner, 1997). After a discussion with Professor William George Penney (Lord Penney) who had previously investigated instabilities in submarine explosions (Penney and Price, 1942), Taylor concluded that it must be due to an instability, with drops being thrown off the water surface as it is disturbed and then returns to its equilibrium position. Only a few days later, Taylor informed Lord Penney that he had solved the problem of the behavior of a modulated plane interface between two fluids in a field of acceleration, which became the original calculation of the Taylor instability (Taylor, 1950). The analytical study of the Taylor instability at a fluid interface accelerating in the direction of the denser fluid was published along with supporting experiments carried out by his research student (Lewis, 1950). This should not be a surprise, as Taylor was a superb experimentalist himself and a strong advocate of the interaction between experiment and theory in fluid mechanics (Taylor, 1974). There is, of course, an equivalence between gravity and acceleration which Taylor recognized – therefore this phenomenon has rightly become known as the “Rayleigh–Taylor instability.”

Sir Geoffrey was described as one of the most notable scientists of the twentieth century (Batchelor, 1994), with many fluid dynamics concepts also bearing his name. “To fluid dynamicists in the world at large, Taylor undoubtedly remains a giant. The centrality of fluid mechanics in Taylor’s research cannot be debated,” according to Sreenivasan (2011).



**Fig. 1.1** Rayleigh–Taylor cirrus clouds. Photograph courtesy of Prof. David Jewitt, University of California at Los Angeles.

Among other things, his contribution is so vast that it provided sufficient material for an entire course at Harvard University, covering topics ranging from hydrodynamic stability and turbulence to electrohydrodynamics and the locomotion of small organisms (Brenner and Stone, 2000).

Early work in the Soviet Union, circa 1950, used a very interesting approach. Mixing at a gravitationally unstable interface between fluids of different density was modeled as turbulent diffusion due to buoyancy-generated turbulence (Belen’kii and Fradkin, 1965). This research was carried out at the Lebedev Institute in Moscow and published posthumously after the death of Belen’kii in 1956. Andronov et al. (1976) considered deceleration by multiple-shocks, rather than by RT, but the Schlieren image was the first image of a “turbulent mixing zone” in this area (Andronov et al., 1976). A shock wave is a discontinuous surface propagating in any elastic medium (such as air, water, or a solid substance) at which density and velocity experience abrupt changes (Courant and Friedrichs, 1948; Zel’dovich and Raizer, 1966; Ben-Dor et al., 2000; Anderson, 2007; Krehl, 2008).

Very little scientific research can be directly linked to the creative world of art, so we should not miss this opportunity to discuss some of these topics as well. Several exquisite paintings of well-known Mexican muralist David Alfaro Siqueiros are created by the artist’s “accidental painting” method (Siqueiros, 1936a,b, 1969; Folgarait, 1987; White, 2009). Unbeknown to him, Siqueiros’ technique of absorption of two or more superimposed colors which infiltrate one another is firmly rooted in fluid physics of the RTI – such “infiltration” or mixing of colors is a direct consequence of an imbalance between the paints’ densities, subject to gravity (Fig. 1.2). Indeed, Zetina et al. (2015) and de la Calleja et al. (2014) have demonstrated that the formation of spotted, patchy areas of contrasting color can be reproduced in a controlled manner (Fig. 1.3). Thus, Siqueiros’ accidental painting technique was not accidental at all (Zenit, 2019).

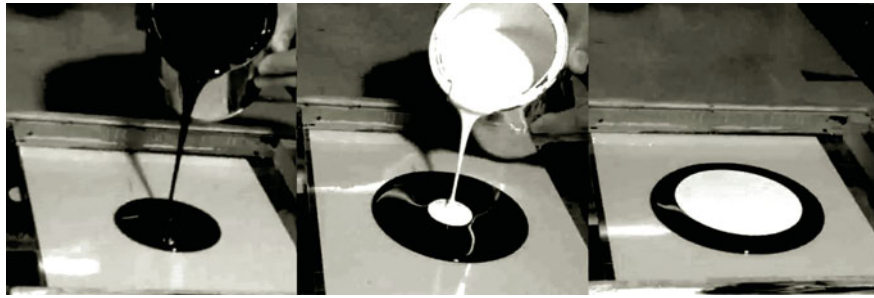
**Fig. 1.2**

Image sequence of the preparation of an “accidental painting” experiment. Fig. 3 of Zetina et al. (2015). Cited in accordance with the Creative Commons Attribution (CC BY) license.

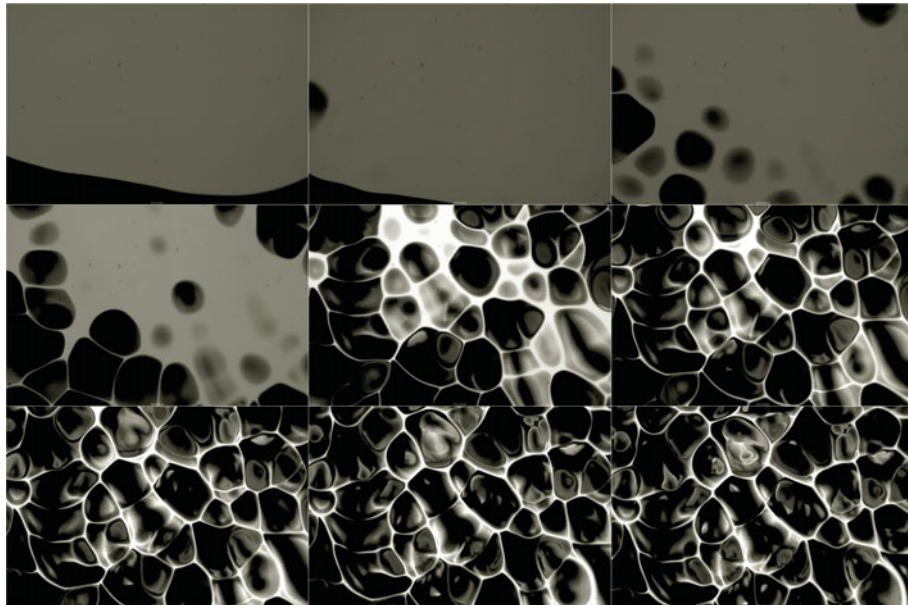
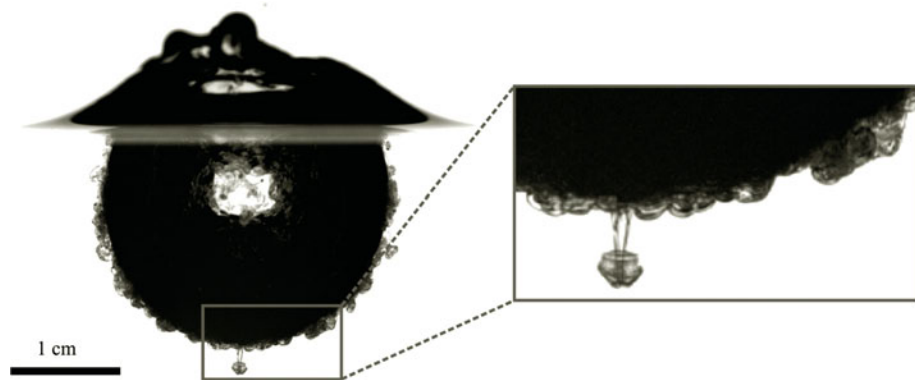
**Fig. 1.3**

Image sequence, white over black paint. The time difference in between frames is 63 s. Time progresses from left to right and from top to bottom. Fig. 5 of Zetina et al. (2015). Cited in accordance with the Creative Commons Attribution (CC BY) license.

At very high-density ratios, for example, water/air, as used in the early RT experiments, the dense fluid forms spikes as it penetrates the lighter fluid (sometimes these structures are described as “fingers”). The lighter fluid “rises” up through the heavier fluid, which in turn “drops” through the lighter fluid. The characteristic structures of the lighter fluid penetrating the heavier fluid are usually referred to as “bubbles,” and the heavier fluid forms “spikes” as it penetrates the lighter fluid. Most notably, “mushroom” shapes form on the spike tips at lower density ratios and for small density differences there is little asymmetry. However, using the terms bubble and spike at all density ratios has persisted in the RT/RM literature.

**Fig. 1.4**

Crater produced by the vertical impact of a liquid drop onto a less dense liquid pool. A spherical RT instability develops around the crater when it decelerates, which results in mushroom-shaped plumes growing radially outward. Lherm et al. (2022).

The RTI is one of the most observed physical processes in nature and in people's daily life. Pouring cream into your morning coffee results in RTI-induced mixing (see the cover image of the book). The spherical RT instability also enters the dynamics of drop impacts when a denser-than-water drop impacts a deep liquid pool of water. Figure 1.4 shows a snapshot from one such experiment, at a time when the impact of the drop has produced a sizeable crater. We see on this picture that the liquid from the drop, which covers the crater floor, has developed mushroom-shaped structures penetrating radially into the water pool (Lherm et al., 2022).

The RT instability of a self-gravitating fluid sphere is important as a mechanism for corona formation on Venus (Hoogenboom and Houseman, 2006) (Fig. 1.5) and in the context of Earth's core formation (e.g., Ida et al., 1989; Mondal and Korenaga, 2017; Sasaki and Abe, 2007; Roy et al., 2024). In a much more violent scenario, asteroid (and/or meteor) RT-instability-induced breakup may be one cause of asteroid (or meteor) swarm impacts in the Venusian atmosphere (Korycansky et al., 2000) (Fig. 1.6) and Earth's atmosphere (Svetsov et al., 1995). The RT-induced perturbation growth and subsequent breakup are dependent on the material strength.

Granular dynamics not only occur in geological applications but also enable technologies ranging from carbon capture to pharmaceutical production (McLaren et al., 2019; Kobayashi and Kurita, 2022). For example, the combination of vibration and upward gas flow through a granular material can produce an analogous process to the RTI. Figure 1.7 shows a time series of optical images of the RTI forming when denser particles are placed initially above lighter particles. Lighter grains start to rise through the heavier grains in fingers (a long thin shape) and "granular bubbles," leaving a trail of particles in their wake (McLaren et al., 2019).

The oceans are dangerous for many creatures. A shrimp (the species *Alpheus heterochaelis*; ~5.5 cm in size, Fig. 1.8) must adopt some unique capabilities to stun and even kill prey animals or to defend a shelter or territory. More specifically, the shrimp issues



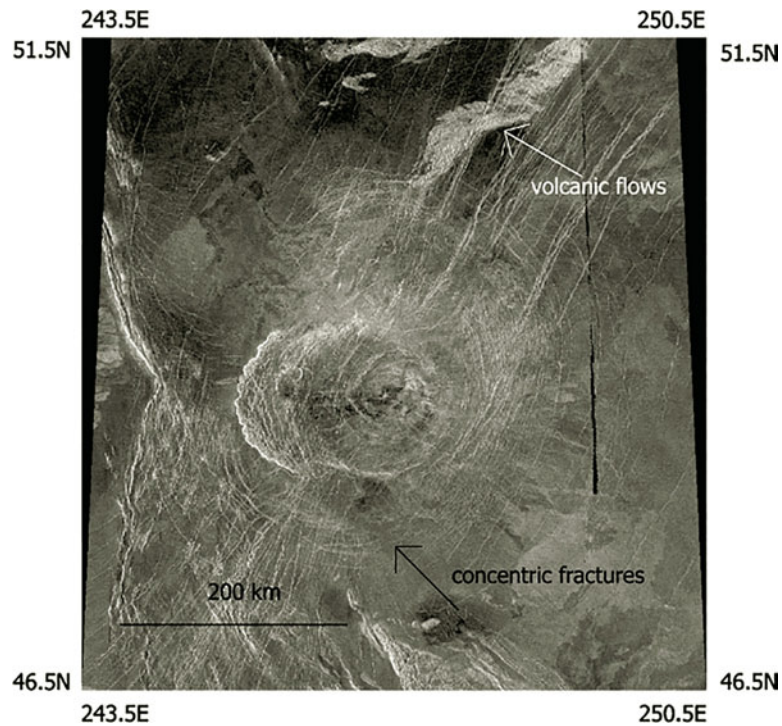


**Fig. 1.5** Magellan synthetic aperture radar image of Nalwomga corona on Venus ( $48.7^\circ\text{N}$ ,  $247^\circ\text{E}$ ). Nalwomga is a concentric, depression-shaped corona (380 km in diameter) located in the plains. Black regions indicate data gaps. Image from <http://pdsmaps.wr.usgs.gov>.

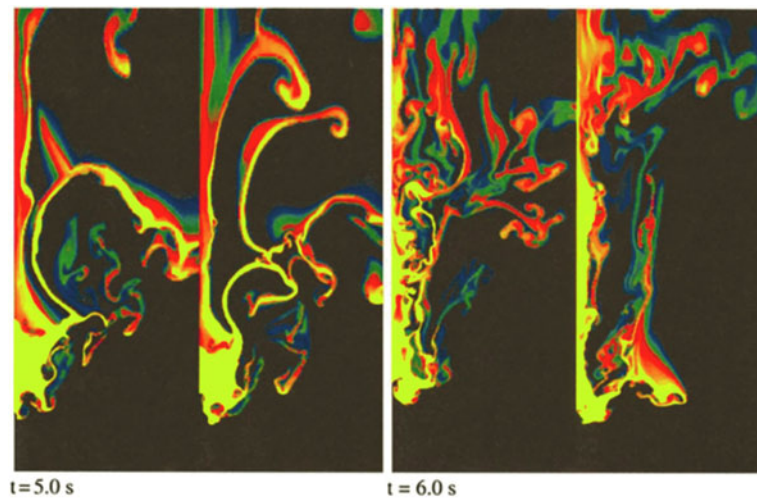


**Fig. 1.6** Asteroid (and/or meteor) Rayleigh–Taylor-instability-induced breakup may be one cause of asteroid (or meteor) swarm impacts. From Korycansky et al. (2000). Reprinted with permission from Elsevier.

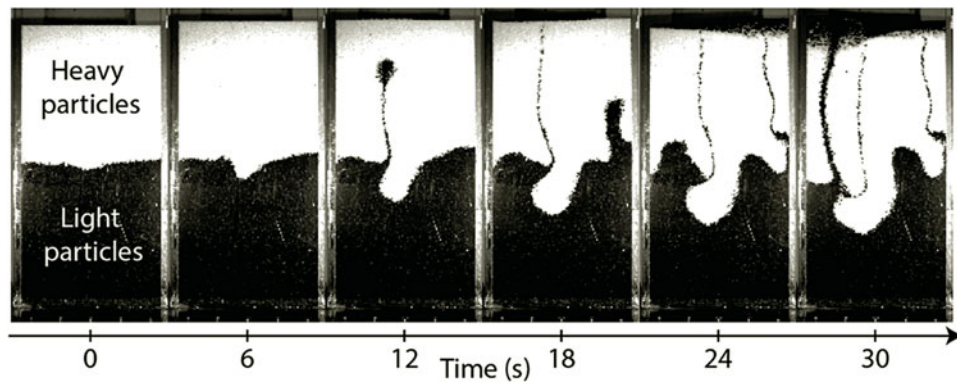


**Fig. 1.7** Time series of optical images of the RT instability forming when denser particles are placed initially above lighter particles. Diameter of light particles:  $1.70 \pm 0.07$  mm; density of light particles:  $2,500 \text{ kg/m}^3$ ; ratio of heavy-to-light particle diameters and densities:  $0.69 \pm 0.03$  and  $2.40$ , respectively. Vibration frequency:  $188 \text{ rad/s}$ . Fig. 1 of McLaren et al. (2019), with permission.

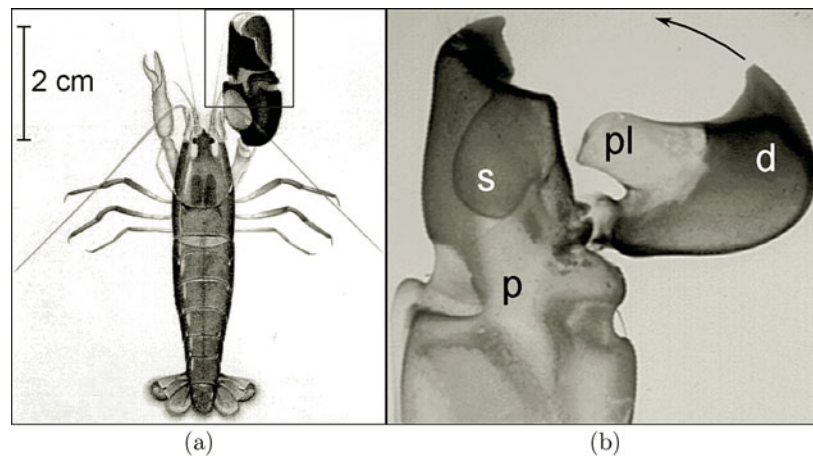


**Fig. 1.8** (a) *Alpheus heterochaelis*, one of the largest snapping shrimp. The large snapper claw may be either on the right or the left in both sexes. (b) Close-up of the snapper claw in its cocked position. The claw is made transparent by the use of methyl salicylate. The claw has a protruding plunger (pl) on the dactyl (d) and a matching socket (s) in the immobile propus (p) (photograph by B. Seibel). Versluis et al. (2000). Reprinted with permission from AAAS.

a high-velocity water jet when the dactyl plunger is driven into the propus socket, displacing water. A cavitation bubble is also created by a water jet formed by an extremely rapid closure of its large snapper claw, which may reach about half of its body size. Studying high-speed images, Versluis et al. (2000) determined that the loud snap is produced through collapse of a cavitation bubble, destroyed through the RTI, instead of that previously attributed to the mechanical contact made when the dactyl and the propus edges hit each other as the claw closes.

The Richtmyer–Meshkov instability (RMI) shares a great many features with the RTI. The RMI arises when a shock wave passes through an interface between two fluids and can be viewed as the impulsive counterpart of the RT instability (i.e., RT with high acceleration for a short time). Recognizing this important insight, Professor Robert D. Richtmyer published the original theoretical analysis of the RMI while he was in residence at Los Alamos National Laboratory (Richtmyer, 1960), during which period he also served as the head of its theoretical division for more than two years. During his next residence at The Courant Institute of Mathematical Sciences, New York University, he moved on to prove the Lax–Richtmyer theorem with Peter Lax, a fundamental theorem in numerical analysis (Lax and Richtmyer, 1956). He eventually settled down at The University of Colorado at Boulder.

Professor Evgeny Evgrafovich Meshkov carried out the first successful isolated experiments of the RMI (Meshkov, 1969) at the All-Russian Scientific Research Institute of Experimental Physics, in Sarov, Russia (also known as Arzamas-16, a closed city long omitted from official maps during the Soviet Union era). Fortunately, Meshkov’s important work became well known worldwide, and the appropriately coined term “Richtmyer–Meshkov instability” has been found in many scientific and engineering applications.

Filling a balloon with water and then throwing it at something (or someone) is a game enjoyed by children both young and old throughout the world (Lund and Dalziel, 2014). The balloon rupture following a collision with a rigid surface, shown in Fig. 1.9, provides an example of the RMI in action. At later times following the balloon rupture, Lund and Dalziel observed a large-scale growth of the interfacial amplitude, where the generation mechanism is momentum in the water due to the preburst waves, a manifestation of the same mechanism that drives the RMI.

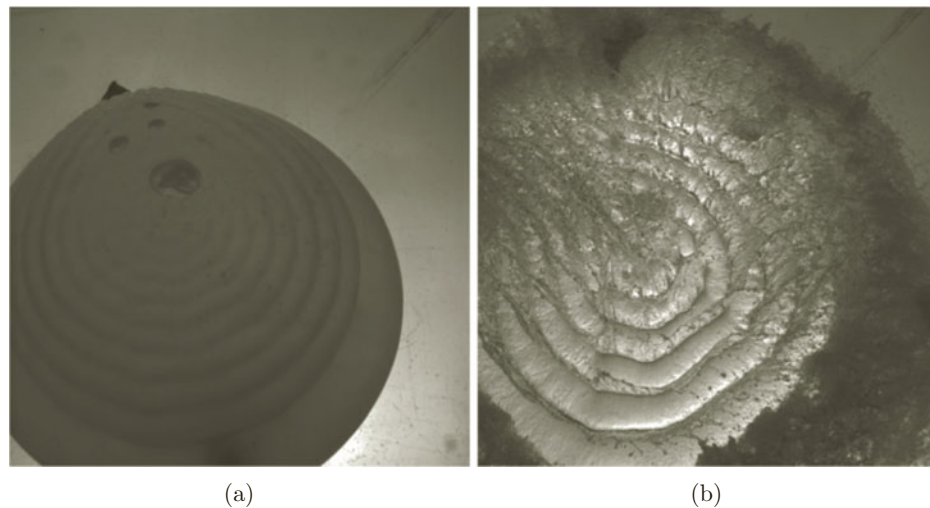
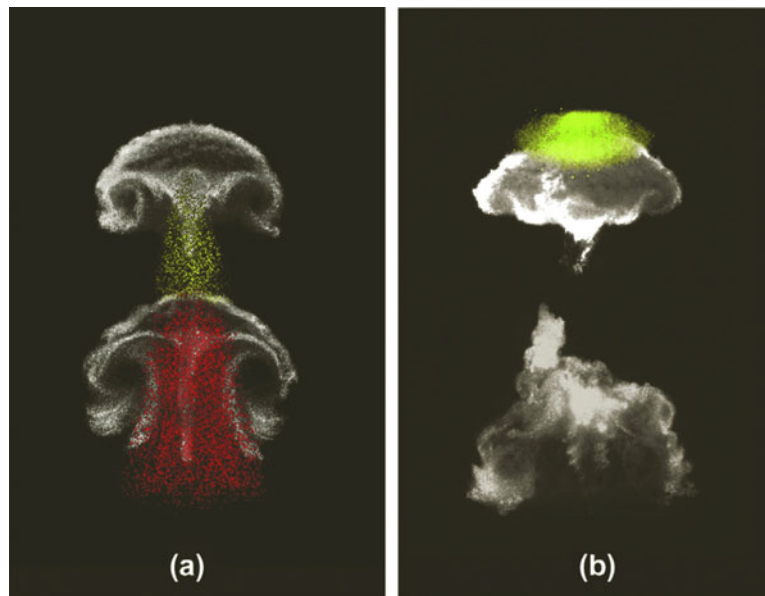


**Fig. 1.9**

The rupturing of a water-filled balloon. (a) The capillary-like waves following a collision with a rigid surface. (b) The Richtmyer–Meshkov-like instability following the removal of the restoring force (i.e., gravity). Lund and Dalziel (2014).

The shock-bubble interaction (SBI) has been considered as a finite-mass, high-interface-curvature analog to the classical RMI (Abd-El-Fattah et al., 1976; Abd-El-Fattah and Henderson, 1978a,b; Bryson and Gross, 1961; Catherasoo and Sturtevant, 1983; Haas and Sturtevant, 1987; Layes and Le Métayer, 2007; Layes et al., 2003, 2005, 2009; Markstein, 1957a,b; Ranjan et al., 2011; Rudinger and Somers, 1960; Singh et al., 2021; Sturtevant and Kulkarny, 1976). A single-shocked (Ranjan et al., 2005, 2007, 2008) or a twice-shocked (Haehn et al., 2010, 2011) spherical gas inhomogeneity has been studied extensively with both shock tube experiments and numerical simulations.

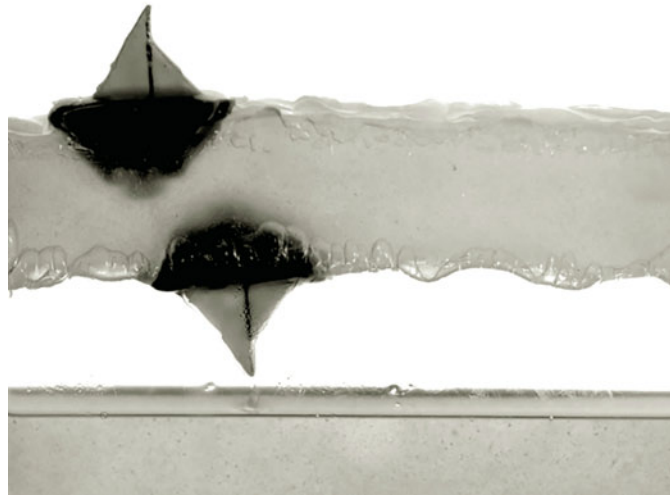
Of particular interest is the fact that depending on the shock strength, the SBI may lead to ignition of chemically reactive gases inside the bubble (Haehn, 2012; Haehn et al., 2012). The reacting shock–bubble interaction (RSBI) allows one to study the interaction between the RMI and the reaction waves inside the bubble that are initiated by the shock (Diegelmann et al., 2016a). Haehn (2012) and Haehn et al. (2012) performed first-of-its-kind RSBI experiments for a range of Mach numbers (Fig. 1.10). Shock focusing leads to an ignition of the bubble gas. Different behaviors from the introduction of reactive gases and variation of the shock strength illustrate why hydrodynamic instability–driven flows are so complex. The numerical work of Diegelmann et al. (2016a,b, 2017) nicely complements that of Haehn et al. These investigations, quite innovative in that they include



**Fig. 1.10**

Composite images showing the development of a shock-accelerated bubble filled with a reactive mixture initially free-falling in  $N_2$ . Each image consists of two chemiluminescence exposures in yellow and red overlaid upon two planar Mie scattering images in grayscale. For clarity, the signal levels have been adjusted and do not reflect the intensity of the chemiluminescence signal. In each image, the incident shock wave travels downward. Haehn et al. (2012). Reprinted with permission from Elsevier.



**Fig. 1.11**

Apffel et al. (2020) levitated a liquid above a layer of air in a container by vertically shaking the container. They observed that objects can float upside down from the lower side of the air–liquid interface. Reprinted with permission from Springer Nature.

chemical reactions, have established an experimental database and a numerical framework for further studies.

Most hydrodynamic instabilities are unwelcome, a prominent example of which are those ones encountered in inertial confinement fusion (ICF). Thus, significant efforts have been devoted to finding mechanisms for suppressing and controlling these instabilities (e.g., Sterbentz et al., 2022; Schill et al., 2024). In a fascinating study that flipped reality on its head, Apffel et al. (2020) succeeded in inducing small boats to float “upside down” based on what has been called “weird physics” (Fig. 1.11). As the authors noted, “[w]hen placed over a less dense medium, a liquid layer will typically collapse downwards if it exceeds a certain size, as gravity acting on the lower liquid interface triggers a destabilising effect called a Rayleigh–Taylor instability.” Impressively, the RTI can be mitigated. The authors demonstrated that vertical shaking can produce a steady rhythm of compressions that maintains the levitating liquid intact and causes bubbles injected into the liquid to be pushed downward, forming an air cushion below the levitating liquid. At the lower interface of the liquid, the vertical shaking also creates stable buoyancy positions, which behave as though the gravitational force were inverted.

While hydrodynamic instabilities are typically detrimental to experimental or engineering designs, enhanced RMI is highly desirable for improving the performance of scramjets (Fig. 1.12), where supersonic air flow into the combustion chamber limits the residence time to a few milliseconds (Marble et al., 1989, 1990; Jacobs, 1992; Yang et al., 1993; Yu et al., 2020; Cao and Michaels, 2022). For flame holdings in supersonic combustion,

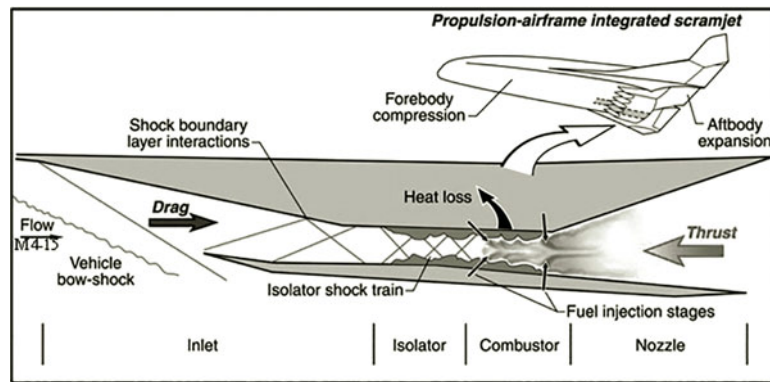


Fig. 1.12

This simplified graphic illustrates how air and fuel mix at supersonic speeds inside a scramjet engine to propel the vehicle to many times the speed of sound. [www.nasa.gov/centers-and-facilities/armstrong/x-43a/](http://www.nasa.gov/centers-and-facilities/armstrong/x-43a/) Credit: NASA.

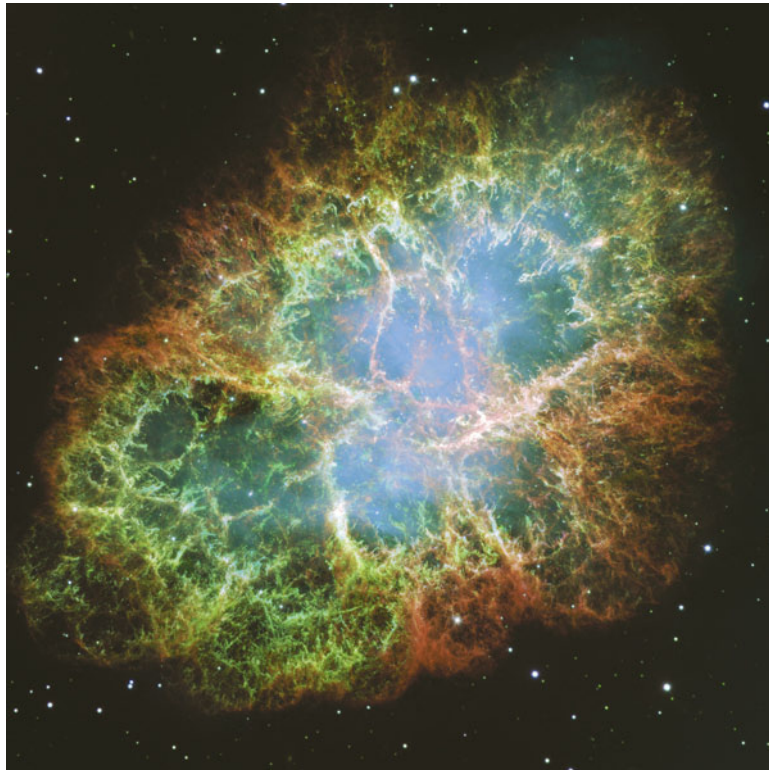
adequate residence time is necessary for atomization, vaporization, mixing and chemical reaction (e.g., Nakaya et al., 2015). The numerical results of Yang et al. (2014) indicate that the RMI phenomenon markedly enhances the mixing efficiency (up to 43%) and is necessary to initiate chemical reactions.

Perhaps the most photogenic examples of hydrodynamic instabilities are the mesmerizing images obtained by the Hubble Space Telescope and other astronomical observational facilities. In fact, RT instabilities are the proposed origin for the filaments of the Crab Nebula; the heavy fluid forms fingers (spikes) that stream downwards while the light fluid forms bubbles that rise between the fingers (Fig. 1.13).

The evolution of the Crab Nebula's bubbles and fingers provides an excellent example of how the RTI or RMI can lead to the development of the Kelvin–Helmholtz instability (KHI), the name given to the instability of two adjacent fluid layers in relative motion. Originally, Lord Kelvin (Sir William Thomson) sought to understand the KHI in the context of the generation of ocean surface waves by wind (Thomson, 1855), while von Helmholtz used this instability to explain the banded clouds (von Helmholtz, 1868).

Figure 1.14 is a photo showing what are known as Kelvin–Helmholtz (KH) clouds over mountains. The KHI has also been observed in the solar atmosphere (Li et al., 2018a; Yuan et al., 2019), and KH billows can be visible at the turbulent boundary between two latitudinal bands in Saturn's atmosphere, which curl repeatedly along the edge (Fig. 1.15).

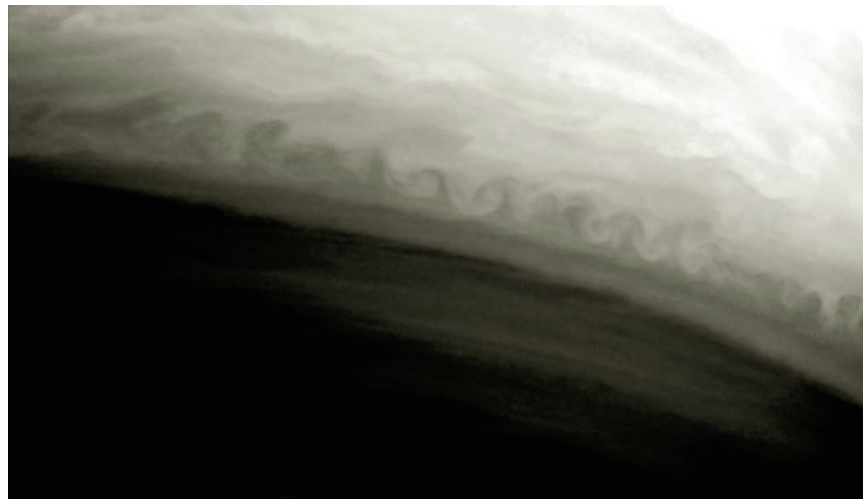
For a challenging measurement, carried out at a depth of half a kilometer in the Atlantic some 700 miles south of the Azores, Van Haren and Gostiaux (2010) used a network of temperature sensors to observe KH billows ripping down the sides of an underwater mountain (Fig. 1.16(a)). While KH instabilities are well observed in the laboratory and nature, the authors still could not resist the temptation to use a definitely nonscientific word “beautiful” to describe this amazing image. Finally, in the deep ocean, van Haren (2015) reported that the RTI penetrates stable density structures under high-frequency internal waves. It arises at the same time as KHI billows emerge at some distance above the slope – see Fig. 1.16(b).

**Fig. 1.13**

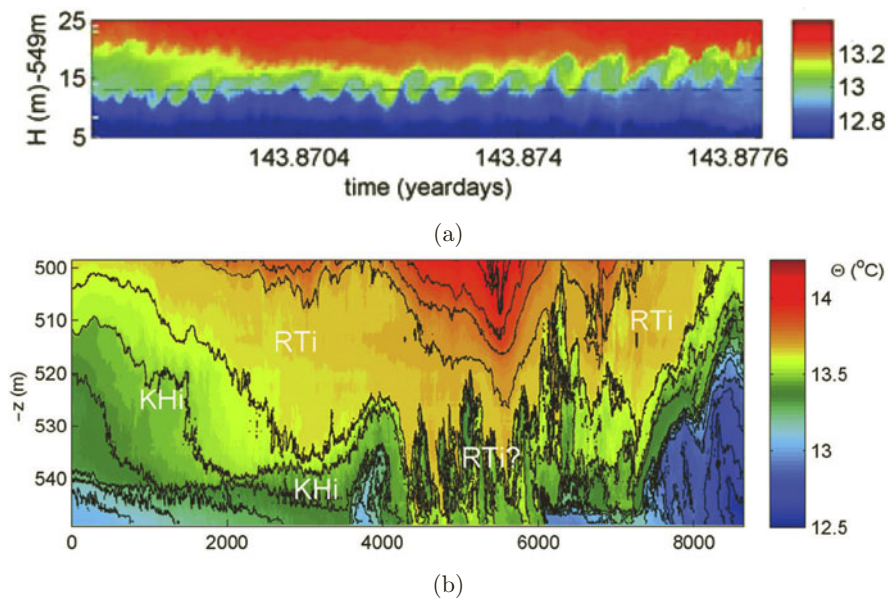
This Hubble image gives the most detailed view of the entire Crab Nebula. It was assembled from 24 individual exposures taken with the Hubble Space Telescope. [www.spacetelescope.org/images/heic0515a/](http://www.spacetelescope.org/images/heic0515a/). Credit: NASA.

**Fig. 1.14**

Kelvin–Helmholtz clouds over the Rocky Mountains. Image: University Corporation for Atmospheric Research, with permission. Photo by Benjamin Foster.

**Fig. 1.15**

This image of Saturn was taken with the Cassini spacecraft narrow angle camera on Oct. 9, 2004, at a distance of 5.9 million kilometers (3.7 million miles) from Saturn. It used a filter sensitive to wavelengths of infrared light centered at 889 nm. [www.jpl.nasa.gov/spaceimages/details.php?id=PIA06502](http://www.jpl.nasa.gov/spaceimages/details.php?id=PIA06502).

**Fig. 1.16**

(a) A deep-ocean Kelvin–Helmholtz billow train. Fig. 3 of Van Haren and Gostiaux (2010). Reprinted with permission from AGU & John Wiley and Sons. (b) High-resolution moored temperature observations above Great Meteor Seamount, Van Haren (2015). Reprinted with permission from Elsevier.

As we will illustrate in Chapters 10–17, the evolution of the RTI and RMI depends on flow properties such as the viscosity, surface tension, and compressibility, as well as on several external factors such as rotation and magnetic field. Moreover, the development of these hydrodynamic instabilities may be strongly affected by the initial conditions. To make the situation more complicated, multiple instabilities appear at the same time in many important scientific and engineering applications.<sup>1</sup> ICF is one such example, the details of which will be investigated in Chapter 19.

From the microscopic to cosmic scales, this manuscript will show that the RT, RM, and KH instability-induced flows and mixing obey the same physical laws and exhibit similar structures and behaviors. The main feature of this work is to strive to treat the RT and RM instabilities in a uniform framework that clearly delineates their similarities and differences.

<sup>1</sup> Over a thousand articles are published each year that are focused on either the physics or applications of RT, RM, and KH instabilities.